Korean J. Chem. Eng., **28**(2), 383-387 (2011)
DOI: 10.1007/s11814-010-0363-8

Electronic density enrichment of Pt catalysts by coke in the propane dehydrogenation

Bao Khanh Vu*, Myoung Bok Song*, Sul-A Park, Youngil Lee**, In Young Ahn***, Young-Woong Suh***, Dong Jin Suh***, Won-Il Kim****, Hyoung-Lim Koh****, Young Gyo Choi****, and Eun Woo Shin*,†**

*School of Chemical Engineering and Bioengineering, University of Ulsan, Daehakro 102, Nam-gu, Ulsan 680-749, Korea
**Department of Chemistry, University of Ulsan, Daehakro 102, Nam-gu, Ulsan 680-749, Korea
***Korea Institute of Science and Technology, Wolsong-gil 5, Seongbuk-gu, Seoul 136-791, Korea
****R&D Business Labs., Hyosung Co., Hoge-dong, Dongan-gu, Anyang, Gyeounggi 431-080, Korea
(*Received 22 April 2010 • accepted 18 June 2010*)

Abstract−We investigated the nature of coke generated in propane dehydrogenation over supported Pt catalysts by FTIR, NMR, and XPS. NMR and FTIR spectra proved that the coke produced in the reaction contained poly-aromatic rings, which was consistent with the previous result that pregraphite-like coke structure was formed. The XPS results indicated that the coke deposits consisted of sp^2 hybridized carbon. All of the characterizations indicated that the pregraphite-like coke containing the poly-aromatic ring structure was generated over the catalysts during the propane dehydrogenation. Furthermore, the XPS measurement demonstrated that the coke deposits interacted with Pt and the electron density of Pt was enriched through the interaction.

Key words: Electronic Density, Propane Dehydrogenation, Coke Deposition, Supported Pt Catalysts, Deactivation

INTRODUCTION

Propane dehydrogenation is an endothermic reaction, and conversion is limited by thermodynamics [1]; commercially viable conversion requires reaction temperatures above 500 °C. At high temperatures, parasitic reactions (such as oligomerization to heavier compounds, cracking to lighter hydrocarbons, skeletal isomerization, aromatization, alkylation of the formed aromatic rings, and formation of coke deposits) lead to rapid loss of activity and lower yields [2]. The optimization of such complex processes requires the characterization of the coke deposits in order to understand the effect of the operational variables on coke deposits and minimize the formation of coke.

Pt/Al_2O_3 and Pt/SBA-15 catalysts have been used for propane dehydrogenation because of their low hydrogenolysis activity [3]. Coke formation on Pt-supported catalysts depends strongly on reaction temperature. At low temperatures, the formation of coke involves mainly condensation and rearrangement steps. However, at high temperatures, the formation of coke involves not only condensation and rearrangement steps but also hydrogen transfer and dehydrogenation steps [4]. The coke mobility on Pt-supported catalysts has been studied through the TPO technique and has been classified into three locations: on Pt metal, on the Pt-support boundary, and on supports. [5,6]. NMR occupies a particularly important technique because of involvement of diverse nuclei and the development of high resolution solid state NMR [7]. The FTIR spectrum shows the CH or CC vibration mode of coke, and the coke structure can be analyzed by XRD and XPS.

There have been many studies on catalytic stability in the propane dehydrogenation [8-11]. However, they focused on decrease in catalytic activity by the coke formation or change in coke mobility due to the interaction of the second metal with Pt. Hence, the papers mainly described coke amounts formed during the reaction by TGA and coke location by TPO [12-14]. In the previous work [15], we observed the different TPO profiles of coke generated over Pt/Al_2O_3 and Pt/SBA-15 catalysts during the propane dehydrogenation and demonstrated that oxygen mobility and coke location on the supports caused the difference in the TPO profiles. In this work, we investigated the nature of the coke formed over Pt/Al_2O_3 and Pt/SBA-15 catalysts in the propane dehydrogenation through FTIR, NMR, and XPS. Furthermore, we provided evidence that the electronic density of Pt was enriched by the interaction with the coke generated on the Pt surface.

EXPERIMENTAL

1. Catalyst Preparation

The mesoporous alumina and SBA-15 support was synthesized by the method described in the previous literature [15,16]. The 3% Pt supported catalysts were prepared using the incipient wetness impregnation technique. The predetermined amount of $H_2PtCl_6 \cdot 6H_2O$ precursor was dissolved in de-ionized water such that its volume was equal to the pore volume of the supports. Then, one aliquot containing 200 μl of precursor was evenly dispersed over the Al_2O_3 and SBA-15 support. This procedure was repeated until the ratio of liquid to support was 1.0 ml/g. Catalysts were dried at room temperature for 24 h in a vacuum hood before drying at 100 °C for 12 h in an oven. The temperature was increased from room temperature to 550 °C with a ramp of 1 °C/min, and the samples were calcined at 550 °C for 6 h. The loading of Pt in each catalyst was 3.0 wt%. Textural properties of the prepared catalysts are listed in Table 1.

With the prepared Pt/Al_2O_3 and Pt/SBA-15 catalysts, dehydrogenation of propane was carried out in a flow reactor at atmo-

†To whom correspondence should be addressed.
E-mail: ewshin@mail.ulsan.ac.kr

Table 1. Textural properties of the support, fresh, and spent catalysts measured by N_2 adsorption-desorption [15]

Catalyst	Surface area (m^2/g)	Pore volume (ml/g)	Pore size (BJH) (nm)
Fresh-3% Pt/Al_2O_3	232.0	0.71	8.40
Spent-3% Pt/Al_2O_3	225.4	0.53	7.53
Fresh-3% Pt/SBA-15	740.3	0.80	5.43
Spent-3% Pt/SBA-15	591.4	0.67	3.67

spheric pressure. The procedure for the reaction and the reaction results including conversion and selectivity for propylene were described in detail in the previous study [15].

2. Characterization

For the spent catalysts, the ^{13}C magic angle spinning (MAS) NMR measurements were performed at room temperature using a Bruker AV3-300 spectrometer (USA) with a 7.05 T magnetic field. For MAS NMR experiments, a 4 mm MAS probe was used with a zirconia rotor at 25.1 MHz for the ^{13}C resonance frequency. The measurements used a 90° pulse length of 4.0 μs, repetition delay of 5 s, spectral width of 30 kHz, and single pulse sequence with 10 k scans. The sample spinning speed was 5 kHz, and all spectra were referenced to adamantane.

An XPS study of fresh and spent catalysts was conducted on a Thermo VG Scientific ESCALAB-250 instrument (UK) with an excitation source of AlK_α radiation. Besides a scan range from 0 to 1,200 eV binding energy for the identification of all detectable elements, detailed scans for chemical state identification and quantification were also obtained. The binding energy of the Al 2*s* (119.0 eV) and Si 2*p* (103.4 eV) line was used as an internal reference for the correction of charging effects in the samples. Because the most intense line of the Pt $4f_{7/2}$ doublet overlaps with the Al 2*p* line from Al_2O_3 support, the spectra were deconvoluted using the Peakfit Ver. 4.12 program.

To improve the sensitivities of the coke bands in the FT-IR measurement, the coked catalyst was treated with a solution of 40% hydrofluoric acid to dissolve the support and to liberate the coke at 25 °C. This method has been validated by P. Magnoux [17], who obtained an unchanged coke structure after treatment. The infrared spectrum of liberated coke was measured in the form of a KBr powder-pressed pellet (120 mg, 1 wt%). The spectrum was recorded by co-adding 124 scans at a resolution of 4 cm^{-1} and a spectral range from 400 to 4,000 cm^{-1} with a Nicolet 380 FT-IR spectrometer (Thermo Electron Co., USA).

RESULTS AND DISCUSSION

In the previous report [15], the 3% Pt/Al_2O_3 and 3% Pt/SBA-15 catalysts lost the conversion and increased selectivity rapidly, as compared to the initial conversion and selectivity for propylene, and it was suggested that a pregraphite-like coke was formed after the reaction on the basis of the XRD patterns. In this study, the spent catalysts were characterized by the sophisticated ^{13}C-CP/MAS NMR technique to further understand the nature of the coke formed during the reaction. Fig. 1 shows the ^{13}C-CP/MAS NMR spectrum of the spent 3% Pt/Al_2O_3 and 3% Pt/SBA-15 catalysts. Interestingly, the coke structure on 3% Pt/Al_2O_3 catalyst is similar to that on 3% Pt/SBA-15 in spite of the different acidity of the supports. In the NMR spectrum, the aromatic nature of coke deposits exhibits the chemical shifts in the region of 120-150 ppm [18]; the chemical shifts in the region of 22-60 ppm (attributable to the aliphatic nature of coke) are almost undetectable [18]. In this study, the ^{13}C-CP/MAS NMR spectrum of coke was also observed at 130 ppm, which is consistent with the results from the dehydrogenation of n-paraffinic C_{10}-C_{13} and the reforming of hydrocarbons over industrial Pt-Sn/Al_2O_3 catalysts [20].

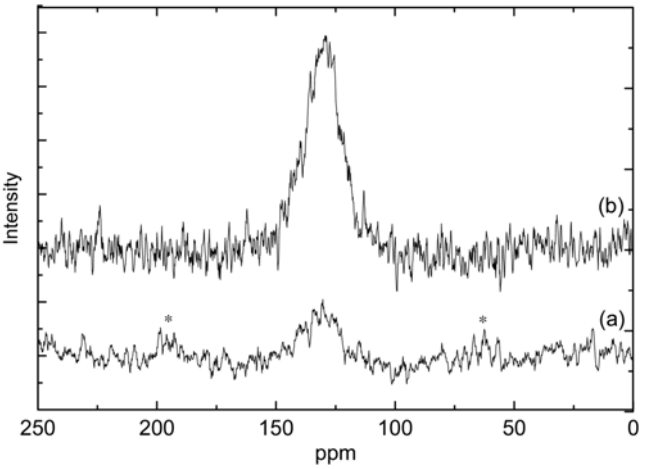

Fig. 1. ^{13}C (CP/MAS) NMR spectra of (a) spent 3% Pt/Al_2O_3 and (b) spent 3% Pt/SBA-15 catalyst after reaction for 160 min. The peaks denoted by an asterisk represent spinning side bands.

Because the coke structure on both catalysts was characterized by XRD [15] and ^{13}C-CP/MAS NMR and they were similar to each other, the liberated coke of spent 3% Pt/Al_2O_3 catalyst was used as a representative for monitoring the coke nature by using FT-IR. A typical FT-IR spectrum of liberated coke is shown in Fig. 2. The spectrum shows a limited number of adsorption bands, which are due to well-defined chemical groups. Two absorption bands at 2,915 and 2,850 cm^{-1} are assigned as alkyl CH stretching. One sharp band at 1,570 cm^{-1} is produced by C=C aromatic/polyaromatic rings. Three bands at 870, 820, and 750 cm^{-1} are interpreted as aromatic CH de-

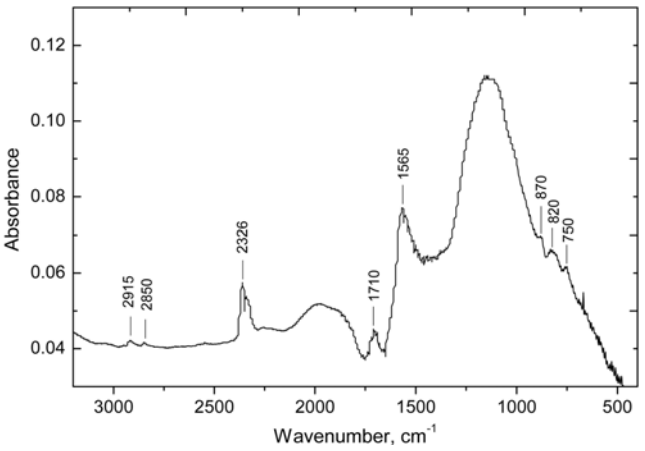

Fig. 2. FT-IR spectrum of librated coke of spent 3% Pt/Al_2O_3 catalyst after reaction for 160 min.

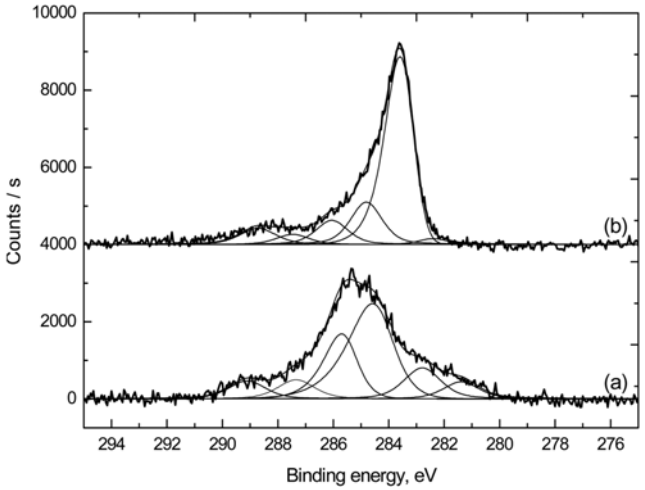

Fig. 3. C1s XPS of (a) fresh 3% Pt/Al_2O_3 and (b) spent 3% Pt/Al_2O_3 catalyst.

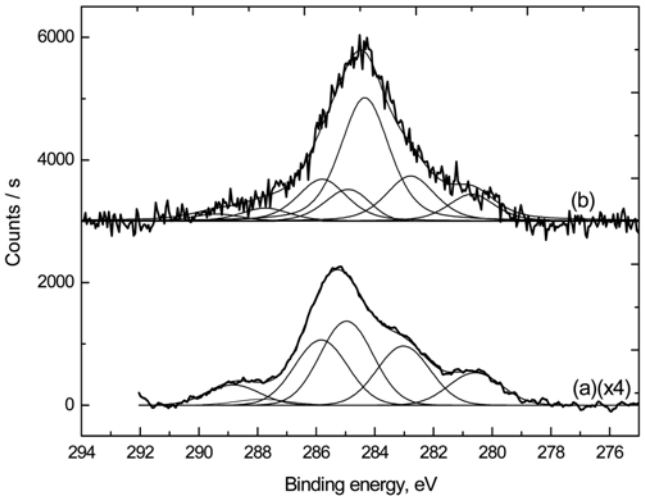

Fig. 4. C1s XPS of (a) fresh 3% Pt/SBA-15 and (b) spent 3% Pt/SBA-15 catalyst.

formation absorptions [21]. Besides, the bands at 1,710 and 2,326 cm^{-1} are due to C=O stretching and atmospheric CO_2, respectively [21].

Figs. 3 and 4 exhibit the C 1s XPS of fresh and spent 3% Pt/Al_2O_3 and 3% Pt/SBA-15 catalysts, and the quantitative data of binding energies and area percentages are summarized in Table 2. Fig. 3 shows the XPS of C 1*s* of the fresh and spent 3% Pt/Al_2O_3 catalysts; one main peak and one broad peak is observed in each case. The C 1*s* region spectra reveal a number of overlapping features corresponding to the varied chemical nature of carbon: aromatic, aliphatic, partially oxidized, and dehydrogenated carbon (DHC). The decomposition of the C 1*s* spectra into individual components was performed, and the binding energies were identified following the previous report [22]. On the fresh catalyst, the two main peaks at a binding energy of 284.58 and 285.70 eV are representative of adventitious hydrocarbon (C-C/C-H) and carbon species in aliphatic polymers (C_xH_y) from contaminants or residues of the template after calcining the as-synthesized catalyst, respectively. Two oxidized carbon species at 287.33 (C=O) and 289.10 eV (O-C=O) were also detected; the peak at 281.38 and 282.32 eV (DHC) is usually observed on the alumina supports after calcination, and this value of binding energy is shifted to the lower one with increasing calcination temperatures [23]. The C 1*s* spectrum of the spent catalyst displays one main peak at a binding energy 283.59 eV, and the asymmetric shape of the peak suggests that the coke deposits consist of the sp^2 hybridized carbon [24]. This type of coke comprises the aromatic rings as observed by NMR and FT-IR techniques, and its lower binding energy than graphitic carbon indicates the high electron density associated with its structure. Carbon species at binding energy <284 eV was previously assigned to platinum carbide Pt-C [25]; however, the formation of Pt-C occurred under much higher temperatures and pressures than those of our experimental conditions [26]. The C 1s binding energy at 283.2 eV was found in the conversion of methane to benzene over Mo/HZSM-5 catalysts and proposed sp hybridization of carbon in coke structure [27]. The binding energy of coke at 283.59 eV was also observed for nickel sulfide catalysts undergoing isobutane dehydrogenation and assigned as graphitic carbon [28].

Table 2. Curve-fitting parameters for C 1s XPS of the fresh and spent catalysts

Catalyst	C 1s					
	DHC*	Pregraphite-like	C-C/C-H	C_xH_y	-C=O	O-C=O
Fresh-3% Pt/Al_2O_3						
BE (eV)	281.38, 282.79	-	284.58	285.70	287.33	289.10
Area (%)	6.6, 12.5	-	43.8	22.1	7.6	7.4
Spent-3% Pt/Al_2O_3						
BE (eV)	282.40	283.59	284.79	285.93	287.85	289.02
Area (%)	1.0	75.8	9.4	5.3	4.6	3.9
Fresh-3% Pt/SBA-15						
BE (eV)	280.58, 283.02	-	284.96	285.83	287.84	288.83
Area (%)	12.1, 22.1	-	31.4	24.4	2.2	7.8
Spent-3% Pt/SBA-15						
BE (eV)	280.70, 282.78	284.34	284.52	285.79	287.73	289.38
Area (%)	9.0, 16.0	43.8	8.8	14.9	4.7	2.8

*Dehydrogenated carbon species

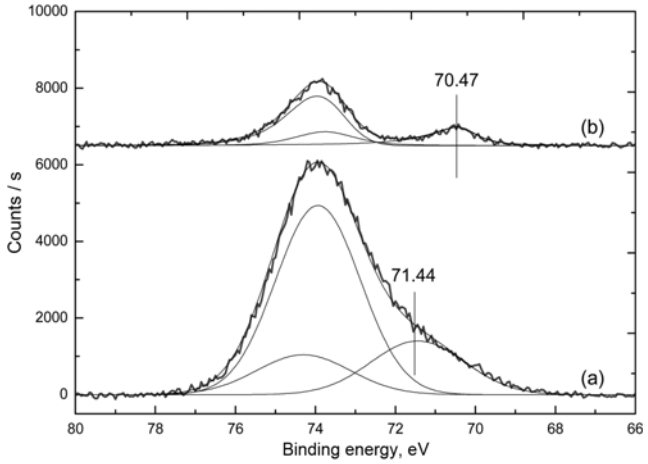

Fig. 5. Pt4f-Al2p XPS of (a) fresh 3% Pt/Al_2O_3 and (b) spent 3% Pt/Al_2O_3 catalyst.

The XPS of C 1*s* from fresh and spent 3% Pt/SBA-15 catalysts are illustrated in Fig. 4. The C 1s spectrum of the fresh 3% Pt/SBA-15 looks similar to that of the fresh 3% Pt/Al_2O_3 catalyst; however, the main peak of the C 1s spectrum at 284.34 eV in the spent catalyst has a higher binding energy than that of the C 1s spectrum in the spent 3% Pt/Al_2O_3 catalyst. This suggests that the coke structure formed over the 3% Pt/SBA-15 catalyst has a lower electron density than that over the 3% Pt/Al_2O_3 catalyst.

Fig. 5 presents the Pt 4*f*-Al 2*p* XPS of the fresh and spent 3% Pt/Al_2O_3 catalysts; the binding energy of Pt $4f_{7/2}$ decreases from 71.44 to 70.47 eV after reacting for 160 min. This observation indicates that coke formed over the spent catalyst has a chemical adsorption and donates electrons to Pt sites; this probably enriches the electron density on Pt sites and, therefore, leads to a decrease in binding energy in the XPS. Our previous study found that this coke had a low oxidation temperature in the TGA profile because of the catalytic effect of Pt metal in oxidation reactions [15]. By using quantum-chemical calculations, Vekki et al. [29] show that the electron density of Pt supported on Al_2O_3 increases significantly when aromatic and poly-aromatic rings chemically adsorb on Pt sites, and, in the case

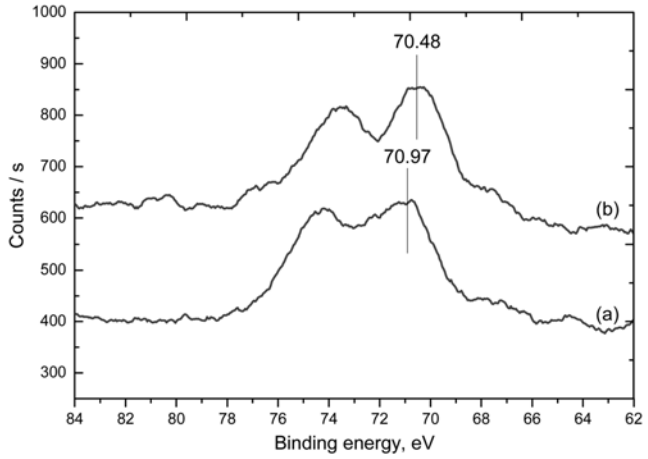

Fig. 6. Pt4f XPS of (a) fresh 3% Pt/SBA-15 and (b) spent 3% Pt/SBA-15 catalyst.

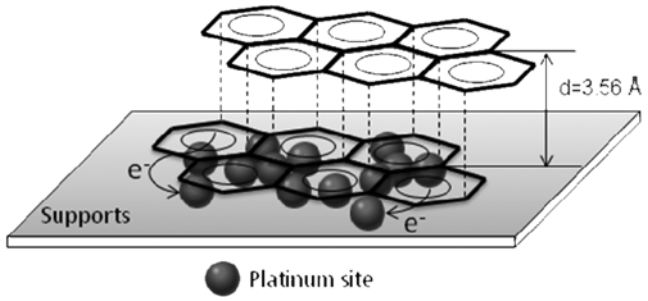

Fig. 7. A schematic diagram for coke-Pt interaction and electron transfer.

of graphitic carbon, the Pt sites gain the richest electron density, comparable to other compounds.

The Pt 4*f* XPS of the fresh and spent 3% Pt/SBA-15 catalysts are shown in Fig. 6. After reaction 160 min on stream, the binding energy of Pt $4f_{7/2}$ on the spent 3% Pt/SBA-15 catalyst is shifted by 0.49 eV when compared with that of the fresh 3% Pt/SBA-15 catalyst; this shifting value in binding energy is smaller than that of 3% Pt/Al_2O_3 (0.97 eV). The observation of Pt $4f_{7/2}$ is consistent with C 1*s* level because the higher electron density structure of coke would lead to higher decrease in binding energy of Pt $4f_{7/2}$ level. Metal-support interaction is stronger between Pt and Al_2O_3 than between Pt and SBA-15 [30]. Moreover, H_2PtCl_6-Al_2O_3 interaction is stronger than H_2PtCl_6-SBA-15 interaction. Since the strong interaction suppresses the mobility of Pt particle, the reduced Pt/Al_2O_3 contains smaller Pt particle size (less electron density) than the reduced Pt/SBA-15 [15]. This effect probably leads to higher binding energy of Pt $4f_{7/2}$ over the reduced Pt/Al_2O_3 than that over the reduced Pt/SBA-15, and similar value of Pt $4f_{7/2}$ over both spent catalysts resulted in smaller shifting in Pt $4f_{7/2}$ over Pt/SBA-15 than that over Pt/Al_2O_3. This similar XPS shift relating to metal-support interaction was also observed over Pd/Al_2O_3 and Pd/SiO_2 [31].

Fig. 7 represents a model for the interaction between the coke generated in the reaction and Pt metals. The coke produced during the reaction is a pregraphite-like carbon, which was proven in previous study [15]. An electron-rich state of the polyaromatic ring in the coke can donate electron to Pt metals, inducing high electron density of Pt metals.

CONCLUSIONS

We systematically investigated the nature of the coke generated in propane dehydrogenation over 3% Pt/Al_2O_3 and 3% Pt/SBA-15 catalysts by FTIR, NMR, and XPS. All the characterizations reveal that the structure of coke deposits consists of poly-aromatic rings with high electron density; coke donates electrons to Pt sites that lead to the shift in binding energy toward lower values in the XPS.

ACKNOWLEDGEMENTS

This work was supported by the Energy Efficiency & Resources program of the Korea Institute of Energy Technology Evaluation and Planning (KETEP) grant funded by the Korea government Ministry of Knowledge Economy (No. 2007MCC24P0230202009).

REFERENCES

1. M. M. Bhasin, J. H. McCain, B. V. Vora, T. Imai and P. R. Pujadó, *Appl. Catal. A*, **221**, 397 (2001).
2. D. Sanfilippo, *CATTECH*, **4**, 56 (2000).
3. S. D. Jackson, G. J. Kelly and G. Webb, *J. Catal.*, **176**, 225 (1998).
4. M. Guisnet and P. Magnoux, *Appl. Catal. A*, **212**, 83 (2001).
5. J. Barbier, E. Churin and P. Marecot, *J. Catal.*, **126**, 228 (1990).
6. O. A. Bariås, A. Holmen and E. A. Blekkan, *J. Catal.*, **158**, 1 (1996).
7. J. L. Bonardet, M. C. Barrage and J. Fraissard, *J. Mol. Catal. A*, **96**, 123 (1995).
8. C. Yu, Q. Ge, H. Xu and W. Li, *Catal. Lett.*, **112**, 197 (2006).
9. G. Aguilar-Ríos, P. Salas, M. A. Valenzuela, H. Armendáriz, J. A. Wang and J. Salmones, *Catal. Lett.*, **60**, 21 (1999).
10. S. R. Miguel, E. L. Jablonski, A. A. Castro and O. A. Scelza, *J. Chem. Technol. Biotechnol.*, **75**, 596 (2000).
11. D. Hullmann, G. Wendt, U. Singliar and G. Ziegenbalg, *Appl. Catal. A*, **225**, 261 (2002).
12. M. Larsson, M. Hultén, E. A. Blekkan and B. Andersson, *J. Catal.*, **164**, 44 (1996).
13. C. Yu, Q. Ge, H. Xu and W. Li, *Appl. Catal. A*, **315**, 58 (2006).
14. Y. Zhang, Y. Zhou, H. Liu, Y. Wang, Y. Xu and P. Wu, *Appl. Catal. A*, **333**, 202 (2007).
15. B. K. Vu, S. Bok, I. Y. Ahn and E. W. Shin, *Catal. Lett.*, **133**, 376 (2009).
16. D. Zhao, J. Feng, Q. Huo, N. Melosh, G. H. Fredrickson, B. F. Chmelka and G. D. Stucky, *Science*, **279**, 548 (1998).
17. P. Magnoux, P. Roger, C. Canaff, V. Fouche, N. S. Gnep, M. Guisnet, B. Delmon and G. F. Froment, *Stud. Surf. Sci. Catal.*, **34**, 317 (1987).
18. E. Breitmaier and W. Voelter, *Carbon-13 Nmr spectroscopy: High-resolution methods and applications in organic chemistry and biochemistry*, Gordon & Breach Science Pub., New York (1987).
19. C. E. Snape, W. R. Ladner and K. D. Bartle, *Anal. Chem.*, **51**, 2189 (1979).
20. N. Martín, M. Viniegra, R. Zarate, G. Espinosa and N. Batina, *Catal. Today*, **107**, 719 (2005).
21. D. W. Mayo, F. A. Miller and R. W. Hannah, *Course notes on the interpretation of infrared and raman spectra*, Wiley-Interscience, New Jersey (2004).
22. E. Desimoni, G. I. Casella, A. Morone and A. M. Salvi, *Surf. Interf. Anal.*, **15**, 627 (1990).
23. G. S. Walker, D. R. Pyke, C. R. Werrett, E. Williams and A. K. Bhattacharya, *Appl. Surf. Sci.*, **147**, 228 (1999).
24. I. Retzko and W. E. S. Unger, *Adv. Eng. Mater.*, **5**, 519 (2003).
25. Z. Paål, R. Schlögl and G. Ertl, *Catal. Lett.*, **12**, 331 (1992).
26. S. Ono, T. Kikegawa and Y. Ohishi, *Solid State Commun.*, **133**, 55 (2005).
27. B. Weckhuysen, M. Rosynek and J. Lunsford, *Catal. Lett.*, **52**, 31 (1998).
28. D. E. Resasco, B. K. Marcus, C. S. Huang and V. A. Durante, *J. Catal.*, **146**, 40 (1994).
29. A. de Vekki, Y. Kraev and A. Solovykh, *Pet. Chem.*, **48**, 210 (2008).
30. M. Arai, T. Ishikawa, T. Nakayama and Y. Nishiyama, *J. Colloid Interf. Sci.*, **97**, 254 (1984).
31. K. Okumura and M. Niwa, *Catalysis Surveys from Japan*, **5**, 121 (2002).